Vol. 16: 283–301, 2024
https://doi.org/10.3354/aei00484

AQUACULTURE ENVIRONMENT INTERACTIONS
Aquacult Environ Interact

Published December 12

Oyster aquaculture enhances sediment microbial diversity: insights from a multi-omics study

Joshua T. E. Stevens[1,5], Nicholas E. Ray[2,3], Alia N. Al-Haj[4,6], Robinson W. Fulweiler[2,4], Priyanka Roy Chowdhury[1,2,*]

[1]Department of Biology, Keene State College, Keene, NH 03435, USA
[2]Department of Biology, Boston University, Boston, MA 02215, USA
[3]Department of Ecology & Evolutionary Biology, Cornell University, Ithaca, NY 14850, USA
[4]Department of Earth and Environment, Boston University, Boston, MA 02215, USA

[5]*Present address:* Department of Biological Sciences, University of South Carolina, Columbia, SC 29208, USA

[6]*Present address:* Smithsonian Environmental Research Center, Edgewater, MD 21037, USA

ABSTRACT: The global aquaculture industry has grown substantially, with consequences for coastal ecology and biogeochemistry. Oyster aquaculture can alter the availability of resources for microbes that live in sediments as oysters move large quantities of organic material to the sediments via filter-feeding, possibly leading to changes in the structure and function of sediment microbial communities. Further, oysters can initiate changes in sediment elemental concentrations, several of which are important mediators of microbial metabolism. Here, we use a chronosequence approach to investigate the impacts of oyster farming on sediment microbial communities over 7 yr of aquaculture activity in a temperate coastal system. We detected shifts in bacterial composition (16S rRNA gene amplicon sequencing), changes in gene expression (meta-transcriptomics), and variations in sediment elemental concentrations (sediment geochemistry) across different durations of oyster farming. Our results indicate that both the structure and function of bacterial communities vary between control (no oysters) and farm sites, with an overall increase in diversity and a shift towards anoxic tolerance in farm sites. However, little to no variation was observed in either structure or function with respect to farming duration, suggesting these sediment microbial communities are resilient to change. We also did not find any significant impact of farming on heavy metal accumulation in the sediments. The minimal influence of long-term oyster farming on sediment bacterial function and biogeochemical processes observed here provides important insights for establishing best practices for sustainable farming in these areas.

KEY WORDS: Oyster farming · Chronosequence · Meta-transcriptomics · Estuary · 16S rRNA · Sediment geochemistry · Sediment bacteria

1. INTRODUCTION

Oysters are filter-feeders that regulate biogeochemical processes in coastal ecosystems by delivering organic material (OM) to sediments and excreting dissolved nutrients. Once common in many coastal systems around the world, natural oyster populations are now only a small fraction of their former historic extent due to overharvesting and diseases (Beck et al. 2011, Zu Ermgassen et al. 2012, Botta et al. 2020). Today, oyster aquaculture is expanding rapidly, particularly on the east coast of the USA (FAO 2018, NMFS 2020). In addition to the economic value of oyster aquaculture, oysters are ecosystem engineers, providing a host of benefits, including habitat provisioning and storm surge protection (Ysebaert et al.

*Corresponding author: pr1043@keene.edu

© The authors 2024. Open Access under Creative Commons by Attribution Licence. Use, distribution and reproduction are unrestricted. Authors and original publication must be credited.

Publisher: Inter-Research · www.int-res.com

2019). Their high filtration capacity (~5 l water h^{-1}) enables them to filter large amounts of particulate matter out of the water. These particles have 2 fates — they can be ingested and deposited to the sediments below as feces; or rejected, wrapped in mucus, and deposited as pseudofeces. The deposition of this OM stimulates a range of microbial processes by changing the availability of compounds used in microbial metabolism (Green et al. 2012), altering oxygen penetration into sediments (Lavoie et al. 2016). This in turn can promote the build-up of chemicals that inhibit certain metabolic pathways (Carlsson et al. 2012, Green et al. 2012). Further, in a simulated lab study, Newell et al. (2002) suggested that most aquaculture-driven changes in nutrient fluxes presumably occur through intermediate microbial processes. Taken together, these studies indicate that the response of sediment microbial communities to the pressure of oyster-mediated OM loading will have important implications for biogeochemistry in the system.

To date, most of the research on the effect of oysters on coastal geochemistry have focused on sediment nitrogen (N) cycling, specifically addressing how oysters alter rates of individual N cycling pathways and the net exchange of various N compounds between the sediment and water column (Ray & Fulweiler 2021). Underlying these changes and individual processes are various microbial guilds that may change in abundance or activity in response to the presence of oysters. For example, oyster farms are considered 'hot spots' for N removal via microbial denitrification (Kellogg et al. 2013, Ray et al. 2021), the microbial conversion of biologically active N to unreactive di-nitrogen (N_2) gas. Microbial denitrification rates are influenced by a variety of factors, including the quality and quantity of OM (Fulweiler et al. 2007, 2013), oxygen concentrations (Nowicki & Nixon1985), and nitrate availability (Nijburg et al. 1997) — all factors impacted by oyster farming (Bouwman et al. 2011, Carlsson et al. 2012). Changes in N cycling can also initiate or coincide with changes in the availability and concentration of carbon (C), phosphorus (P), and sulfur (S) (Burgin et al. 2011). In areas of high OM deposition, such as beneath oyster cages, hydrogen sulfide (H_2S) can build up, subsequently inhibiting rates of nitrification and denitrification (Asami et. al. 2005, Holmer et al. 2005). In addition to altering availability of these 4 elements (C, N, P, and S), oyster-mediated OM loading can enhance the availability of heavy metals (such as copper [Cu], zinc [Zn], and lead [Pb]; Smith et al. 2005, Mendiguchía et al. 2006, Sutherland et al. 2007) and trace metals (such as arsenic [As], cadmium [Cd], cobalt [Co], chromium [Cr], iron [Fe], manganese [Mn], and nickel [Ni]; Boothe & Knauer 1972, Silva et al. 2018), several of which are required by enzymes that perform microbial metabolism. For example, enzymes important for denitrification, such as nitrate reductase, requires a molybdenum (Mo) protein cofactor for reducing nitrate to nitrite (Ge et al. 2019), and nitrous oxide reductase requires Cu for reducing nitrous oxide (N_2O) to N_2 (Scala & Kerkhof 1999). The concentration of Fe has a significant role in mediating the microbial mobilization of Fe-bound P in marine sediment (Pettersson 1998). Therefore, it can be assumed that any changes in the environmental supply of these metals (e.g. Mo, Cu, and Fe) could significantly impact the cycling of other nutrients (e.g. N and P) (Hussain et al. 2020). Considering the effect of oyster farming on both the availability of metals and the microbial communities is an important next step toward broader insights into how oysters regulate biogeochemical processes across systems.

Past studies have investigated how sediment microbial communities may differ between oyster habitats and nearby areas without oysters. For example, Feinman et. al. (2018) demonstrated higher bacterial abundance beneath oyster aquaculture compared to bare sediment and there is also evidence for significant shifts in communities following implementation of other types of shellfish culturing (Asami et al. 2005, Richardson et al. 2008, Liu et al. 2023). While these studies provide insight into how sediment communities may change following introduction of shellfish aquaculture, they have focused on the dynamics of a few well-characterized microbial groups, and do not capture the complexities in communal shifts in both structure and function in response to farming over time. Nor do they capture the impact of related elemental biogeochemical processes that are important for controlling the microbial-driven nutrient cycles in sediments.

Bacteria can respond promptly to changes in their environment due to shorter generation time allowing faster rates of evolutionary changes. For example, bacterial communities in restored salt marshes have been found to resemble those of reference salt marshes before there was evidence of plant growth (Lynum et al. 2020), making bacterial communities effective ecological indicators. Given the potential for rapid microbial evolution, community composition alone may not accurately capture all functional variations that arise in response to environmental impacts. Therefore, an integrative approach comparing community-wide changes in structure and function of bacteria is vital for a holistic understanding of the extent of farming impacts, which in turn can be useful in future monitor-

ing and management of these farms. In the present study, we use a multi-omics approach to assess shifts in sediment bacterial communities along an oyster aquaculture 'chronosequence' (space-for-time substitution, Ray et al. 2020). To that end, we first used 16S rRNA gene amplicon sequencing to characterize changes in the structure and function of bacterial communities in bare sediments and sediments beneath oyster farms of various ages. Then we used RNA metatranscriptomics to identify similar community shifts in response to oyster farming. Using both DNA and RNA sequencing allowed us to detect changes in the 'potential' (16S rRNA gene) compared to the 'active' (mRNA) shifts in response to farming. Finally, we measured changes in sediment elemental concentrations in relation to the age of oyster farming to identify the effects of farming on elements beyond N, C, P, and S. We hypothesized that there would be significant changes in both the structure and function of the bacterial community in response to farming duration due to changes in both biotic and abiotic factors induced by the oysters. Meta-transcriptome data allowed us to identify specific bacterial processes and their associated functions that mediate the above shifts in composition. Based on previous studies (Tovar et al. 2000, Rožič et al. 2012), we predict greater accumulation of metals (e.g. Cd, Cu, Pb, Zn) at farmed sites due to OM deposition by the oysters.

2. MATERIALS AND METHODS

2.1. Study site and sample collection

Sediments were collected from Ninigret Pond (41.357° N, 71.653° W), a coastal back barrier lagoon located in southern Rhode Island, USA (Fig. S1 in the Supplement at www.int-res.com/articles/suppl/q016p283_supp.pdf). Four sites were selected within a commercial oyster farm (0.016 km^2) in the lagoon that employs a rack and bag technique, where oysters *Crassostrea virginica* are held in plastic mesh bags suspended approximately 10–20 cm from the sediment surface on PVC racks. Different portions of the farm had been in use for varying lengths of time (0, 3, 5, and 7 yr) that corresponded to a chronosequence (space-for-time substitution). The 0 yr old or control site was located on bare sediment approximately 10 m upstream of aquaculture gear but still on the farm. Water depth across sampling sites was about 1 m and sites were at least 15–20 m apart from each other. In June 2015, duplicate sediment samples were collected using a 25 mm corer from the top 1 cm of sediments under oyster cages from 3 benthic chambers (>1 m apart) within each of the 4 sites, yielding 24 total samples. Sediment samples were placed on dry ice, transported back to the laboratory, and stored at −80°C until downstream analyses. A more detailed description of the study location, oyster farming approach, and methods for sample collection can be found in Ray et al. (2020).

2.2. DNA extraction and analyses

We used 16S rRNA gene amplicon sequencing to identify changes in bacterial community composition based on the protocol described in Stevens et. al. (2019). Briefly, DNA was extracted using the Qiagen DNeasy PowerSoil Pro Kit (cat. no. 47014). Purified DNA was then shipped to MR DNA (Shallowater, TX, https://www.mrdnalab.com/) for sequencing on an Ion Torrent personal genome machine (PGM) after PCR amplification of the 16S rRNA V4 region with primers 515F and 806R (Caporaso et al. 2011). Initial quality control of sequences was done using the MR DNA analysis pipeline to remove primers, barcodes, and any sequences <150 bp. A 97% similarity cutoff was applied to filtered reads to identify operational taxonomic units (OTUs), and chimeras were removed using a modified UCHIME algorithm (Edgar et al. 2011). OTUs were clustered using USEARCH and classified using BLASTN against databases derived from the Ribosomal Database Project II (v. 11.5, http://rdp.cme.msu.edu, Cole et al. 2014) and NCBI database (https://www.ncbi.nlm.nih.gov, accessed August 8, 2018) using default settings (Glassing et al. 2015, Schmidt et al. 2018).

2.3. RNA extraction and analyses

We isolated RNA from 6 sediment samples (3 replicates each from the control and 7 yr old site). The 7 yr site was chosen as it had the longest duration of farming compared to the other sites. RNA from all 6 samples were extracted from ~2 g of sediment using the Qiagen RNeasy PowerSoil Total RNA Kit (cat. no. 12866) following the manufacturer's protocol. RNA was quantified using the Qubit RNA HR assay kit (Thermo Fisher Scientific) in a Qubit Fluorometer (Thermo Fisher), before shipping to the UNH Hubbard Center for Genome Studies for sequencing (https://hcgs.unh.edu/). Following the manufacturer's protocols, RNA was first reverse-transcribed using the SuperScript Double-Stranded cDNA Syn-

thesis Kit (Thermo Fisher) followed by construction of RNA libraries using the Illumina-compatible Nextera DNA Flex Library Prep Kit (cat. no. 20018705). Illumina-compatible adapters from the Nextera DNA Unique Dual Indexes (cat. no. 20027213) were used to attach individual barcodes to all 6 libraries. Library size distribution was determined using a Bioanalyzer 2100 (Agilent Technologies) with DNA High-Sensitivity chips and reagents (Agilent Technologies). Illumina TruSeq SBS v4 reagent kit (300 cycles) was used to generate paired-end 150 bp reads using the Illumina HiSeq platform. The initial quality check was done with FastQC (v.0.11.6) (https://www.bioinformatics.babraham.ac.uk/projects/fastqc). Low-quality reads and TruSeq3-PE adapters were then removed in Trimmomatic (v. 0.27) using default settings (Bolger et al. 2014). Trimmed and filtered reads were uploaded to the MG-RAST API server (http://metagenomics.anl.gov, Meyer et al. 2008) for both taxonomic and functional analyses of MetaT data following previously established protocol (Urich et al. 2008, Yu & Zhang 2012). Briefly, RNA was first converted to cDNA. A minimum e-value $<1\ e^{-5}$ and 60% identity cut-off were used for database searches within MG-RAST. RefSeq database was used to tabulate rRNA transcript counts at each taxonomic level, and mRNA transcripts were annotated with SEED Subsystem and visualized using KEGG (an internal tool based on the Kyoto Encyclopedia of Genes and Genomes pathway mapping system).

2.4. Metal extraction and analyses

Thawed sediments from each of the 24 sediment samples were ground to a fine powder using a mortar and pestle. Approximately 2 g of each dried and thawed sample was then sent to the Trace Metal Analyses Core at Dartmouth College to measure elemental concentrations using an Agilent™ 7900 inductively coupled plasma mass spectrometer (ICP-MS). Prior to analysis, samples were digested in a 5 ml HNO_3:HCl (9:1) mixture and heated at 110°C for an hour. On cooling, 45 ml of DI water was added before running in the ICP-MS with a commercial internal standard mix for calibration purposes.

2.5. Statistical data analyses

All analyses were performed in the statistical platform R (v. 4.2.1; R Core Team 2017) using the RStudio interface (v. 2023.09.1+494; RStudio Team 2020), including the vegan (Oksanen et al. 2013), ggplot2 (Wickham 2009), and DESeq2 (Love et al. 2014) packages. The 'rarefy' function in the vegan package was used to test for adequate sequencing depths across amplicon samples prior to any analyses. Alpha diversity (Shannon and Chao1 indices) was evaluated using the vegan package, and 1-way ANOVA followed by Tukey's post hoc tests was used to measure differences between sites. To meet the assumptions of ANOVA, the residuals were plotted graphically to confirm normal distribution and the Levene test was used to confirm equality of variances in R. Beta diversity (sample clustering) was visualized using non-metric multidimensional scaling (nMDS) ordination on relative abundances (to account for differences in sequencing depth across samples) using the Bray-Curtis dissimilarity matrix in vegan (k = 2; trymax = 50). Significance of microbial community shifts between sites was tested using PERMANOVA with the 'adonis ()' function, followed by pairwise comparison between sites using the 'pairwise.adonis2()' function in the vegan package. Linear discriminant analysis (LDA) effect size (LEfSe) analysis was used to detect site-specific bacterial markers using LEfSe of Galaxy of the Huttenhower lab (Segata et al. 2011). Potential bacterial functions were identified from the 16S rRNA data using PICRUSt (Langille et al. 2013) in Qiime2 (Bolyen et al. 2019). Differential abundance in KEGG functional pathways between the control and farmed sites were determined in ggpicrust2 (Yang et al. 2023) using ALDEx2 (Fernandes et al. 2013) that uses the Wilcoxon rank test for statistical significance between treatments. All predictions were corrected for multiple testing (Benjamini-Hochberg method, FDR $q<0.05$).

For RNA sequencing, KEGG-annotated gene counts and RefSeq-based taxonomic counts were used for nMDS ordination using a Bray-Curtis dissimilarity matrix, followed by PERMANOVA analyses for site-specific differences. Reads per million (RPM) transformation was done prior to testing to account for differences in sequencing depth across samples. Differential gene expression of KEGG transcripts between the control and the 7 yr site was calculated using DESeq2 (Love et al. 2014). Results were plotted in SRplot (www.bioinformatics.com.cn/srplot). Diversity indices of RNA-derived taxonomic profiles were calculated using vegan, and a Student's *t*-test was used to test for differences between sites. To test for similarity between community composition derived from DNA and RNA sequences, 2-tailed Student's *t*-tests were performed on Canberra pairwise community distances at the phylum level using the 'vegdist' function in vegan (see Meyer et al. 2019).

For sediment elemental concentrations, nMDS based on a Bray-Curtis dissimilarity matrix were performed on *z*-transformed data to normalize distributions across samples, followed by PERMANOVA to test for differences among sites. Pearson's correlation analysis using the 'stats' package was used to assess associations between elements. Individual concentrations of elements were compared across sites using a 1-way ANOVA followed by Tukey's post hoc tests. The Levene test was used to confirm equality of variances for individual elements. The contribution of elements to variations in the bacterial community was estimated by distance-based redundancy analyses (db-RDA) using the 'rda()' function in vegan using default settings. Only elements that showed a significant correlation with grouped samples using the 'envfit' function in vegan were used in the redundancy analyses (Oksanen et al. 2013).

3. RESULTS

3.1. DNA community structure and function

16S rRNA gene amplicon sequencing in all 24 samples (4 sites × 6 replicates) showed a mean (±SD) of 58 137 ± 15 636 sequences sample^{-1} (Stevens et al. 2019). We identified 13 147 OTUs belonging to 53 phyla, 119 classes, and 1137 genera across samples. Rarefaction curves (Fig. S2A) indicate that most samples had comparable sequencing depth, with all 3 yr replicates showing greater OTU abundances compared to the rest. Control, 5 yr, and 7 yr farm sediment replicates had nearly equal abundances, but the control replicates exhibited lower species diversity than the farmed sites (Fig. 1A, Table 1). These findings were also supported by diversity indices analyses, where control samples were significantly less diverse than all 3 farmed sites (Shannon: $F_{3,20}$ = 15.92, p < 0.001; Chao1: $F_{3,20}$ = 12.12, p < 0.001), with Tukey's post hoc test revealing no variation between the 3, 5, and 7 yr sites (Table 1, Fig. 1A, Fig. S2B). nMDS ordination was used to examine clustering at the OTU levels where control samples clustered separately from other farmed sites. Three and 5 yr sites clustered closer compared to 7 yr sites (Fig. 1B). PERMANOVAs indicated a significant difference between control and farmed sites at the OTU level (pseudo-$F_{3,23}$ = 3.2063, p = 0.001). Post hoc pairwise comparison showed differences between the control and the 3 yr (p = 0.006), 5 yr (p = 0.024), and

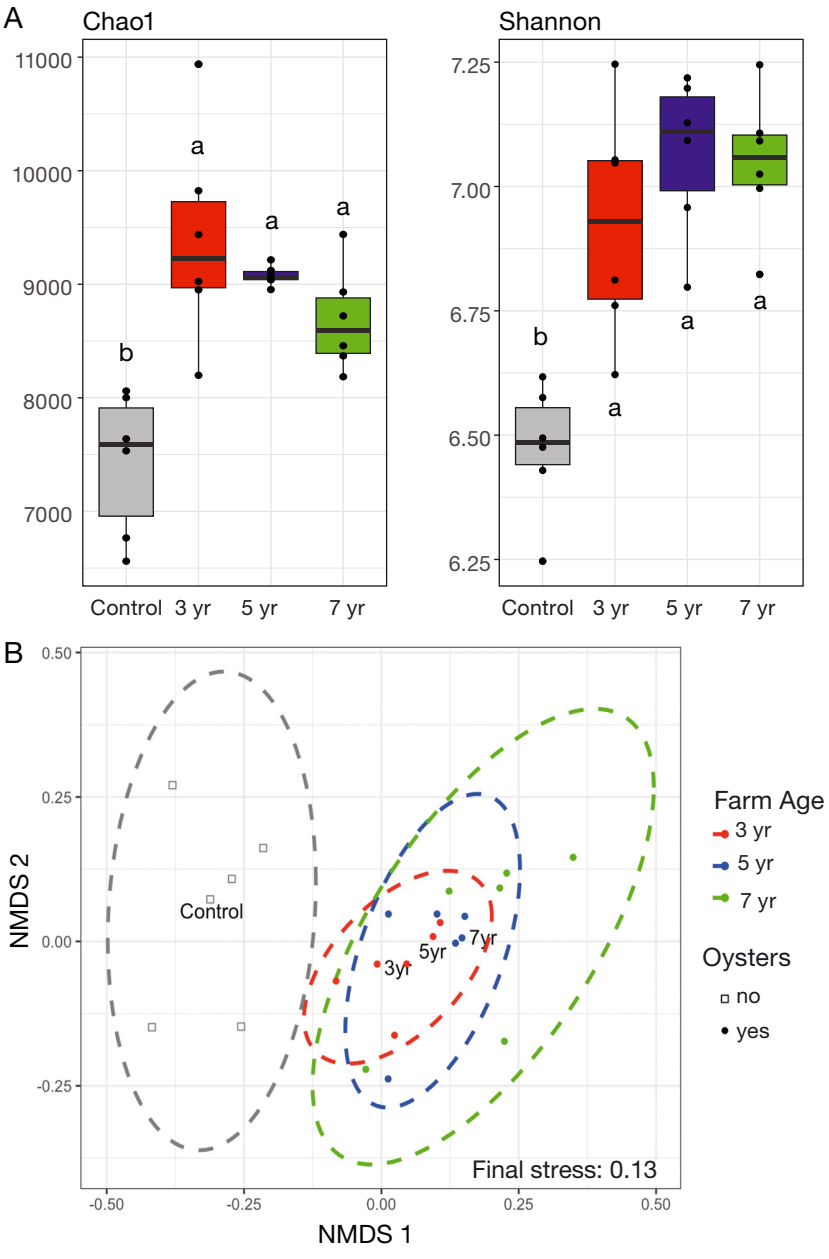

Fig. 1. (A) Chao1 and Shannon diversity analyses and (B) non-metric multidimensional scaling (nMDS) of 16S rRNA sediment bacterial community based on operational taxonomic unit. Horizontal line, boxes, and whiskers represent the median, interquartile range, and mild outliers, respectively. Single point denotes outliers. Different letters denote significant differences in diversity

Table 1. 16S rRNA gene and Illumina HiSeq sequencing output showing total sequences obtained in each, number of operational taxonomic units (OTUs) and KEGG annotations in 16S rRNA and HiSeq mRNA respectively, and diversity indices (Chao1 species richness estimator and Shannon's diversity index) of OTU abundances across the 24 sample sites

Samples		Sequencing results			Diversity indices	
ID	Replicates	Total sequences	Total OTUs	Total RNA sequences	Chao (Adj. mean ± SE)	Shannon
OA 1 (3 yr)	1	60222	5247		8198.05 ± 169.60	6.622
	2	77498	6041		8950.67 ± 159.59	6.761
	3	79364	6790		9823.40 ± 159.05	7.054
	4	55986	5490		9024.79 ± 198.32	6.812
	5	110642	8039		10937.86 ± 146.27	7.246
	6	62602	6219		9437.60 ± 172.66	7.047
OA 2 (5 yr)	1	55220	6192		9214.86 ± 162.42	7.198
	2	54207	5992		9040.73 ± 163.92	7.092
	3	60933	6233		9122.10 ± 155.28	7.128
	4	59288	5896		9040.76 ± 171.81	6.797
	5	58102	6234		8953.25 ±144.97	6.958
	6	54910	6174		9080.96 ± 155.96	7.218
OA 3 (7 yr)	1	56817	5668	83269256	8458.50 ± 155.37	6.996
	2	58693	6184	36621730	9438.57 ± 175.81	7.245
	3	44746	5192	35363476	8185.34 ± 172.14	7.025
	4	51093	5497		8721.45 ± 178.72	6.823
	5	61428	5920		8931.89 ± 167.27	7.092
	6	36178	5070		8568.98 ± 188.78	7.107
Control (0 yr)	1	40191	4223	35075482	6765.94 ±160.72	6.247
	2	68971	5354	89208186	8059.65 ± 157.38	6.429
	3	62123	5208	57674984	8001.22 ± 161.84	6.576
	4	41123	4690		7638.55 ± 173.16	6.476
	5	39511	3990		6561.23 ± 166.65	6.494
	6	45612	4849		7533.02 ± 159.28	6.617

7 yr ($p = 0.030$) sites, but no significant differences between the 3 farmed sites. Bacterial groups that are more likely indicators of this difference were characterized by LEfSe that revealed that 13 OTUs were enriched in the farmed sites (3, 5, and 7 yr, LDA scores 3.4–5.3) and 14 OTUs were enriched in the control samples (LDA scores 2.7–5.6) (Fig. 2A, Fig. S3). Taxa enriched in farm sites belonged to the phylum *Proteobacteria*, except 1 that belonged to *Firmicutes.* Within *Proteobacteria*, 11 belonged to the class *Deltaproteobacteria* and 1 to *Epsilonproteobacteria*. *Desulfobacterales* and *Desulfuromonadales* were the 2 enriched orders in the farm sites. In the control site, the phyla *Proteobacteria* (8), *Bacteroidetes* (5), and *Spirochaetes* (class *Spirochaetia*) (1) were enriched (Fig. S3). Within *Proteobacteria*, the class *Alphaproteobacteria* (order *Rhodobacterales*) showed the highest LDA score, followed by *Gammaproteobacteria*. Within *Bacteroidetes*, class *Sphingobacteriia* (order *Sphingobacteriales*) had the highest LDA score, followed by *Cytophagia* (order *Cytophagales*) (Fig. 2A, Fig. S3).

Phylum-level abundances across the 4 sites were published previously in Stevens et al. (2019). Several classes within the 4 most abundant phyla (*Proteobacteria*, *Bacteroidetes*, *Firmicutes*, and *Chloroflexi*) showed variations among the 4 sites (Fig. 2B). For example, within *Proteobacteria* (graph I in Fig. 2B), *Deltaproteobacteria* abundance increased from 11 to 28% ($F_{3,30} = 20.699$, $p < 0.001$), while *Gammaproteobacteria* decreased (19 to 14.8%) from control to 7 yr sites ($F_{3,30} = 8.803$, $p < 0.001$). Within *Bacteroidetes* (graph II in Fig. 2B), both *Cytophagia* (4 to 8%) and *Bacteroidia* (0.7 to 2.6%) had higher abundances at the 7 yr site compared to the control site. The most dramatic increase in abundances was seen in *Firmicutes* (graph III in Fig. 2B), where both *Bacilli* (0.4 to 1.8%) ($F_{3,30} = 10.136$, $p < 0.001$) and *Clostridia* (0.9 to 3.3%) ($F_{3,30} = 15.418$, $p < 0.001$) increased significantly with years of exposure to oysters. *Chloroflexi* (graph IV in Fig. 2B) showed little variation between control and farmed sites, with only *Chloroflexia* (0.07 to 0.13%) ($F_{3,30} = 4.719$, $p = 0.012$) showing a significant increase in 7 yr farm sites. Among the top 100 most abundant genera (Fig. S4), several were extremely less abundant (<1%) at the control site, but abundance was higher (>8%) with duration of farming

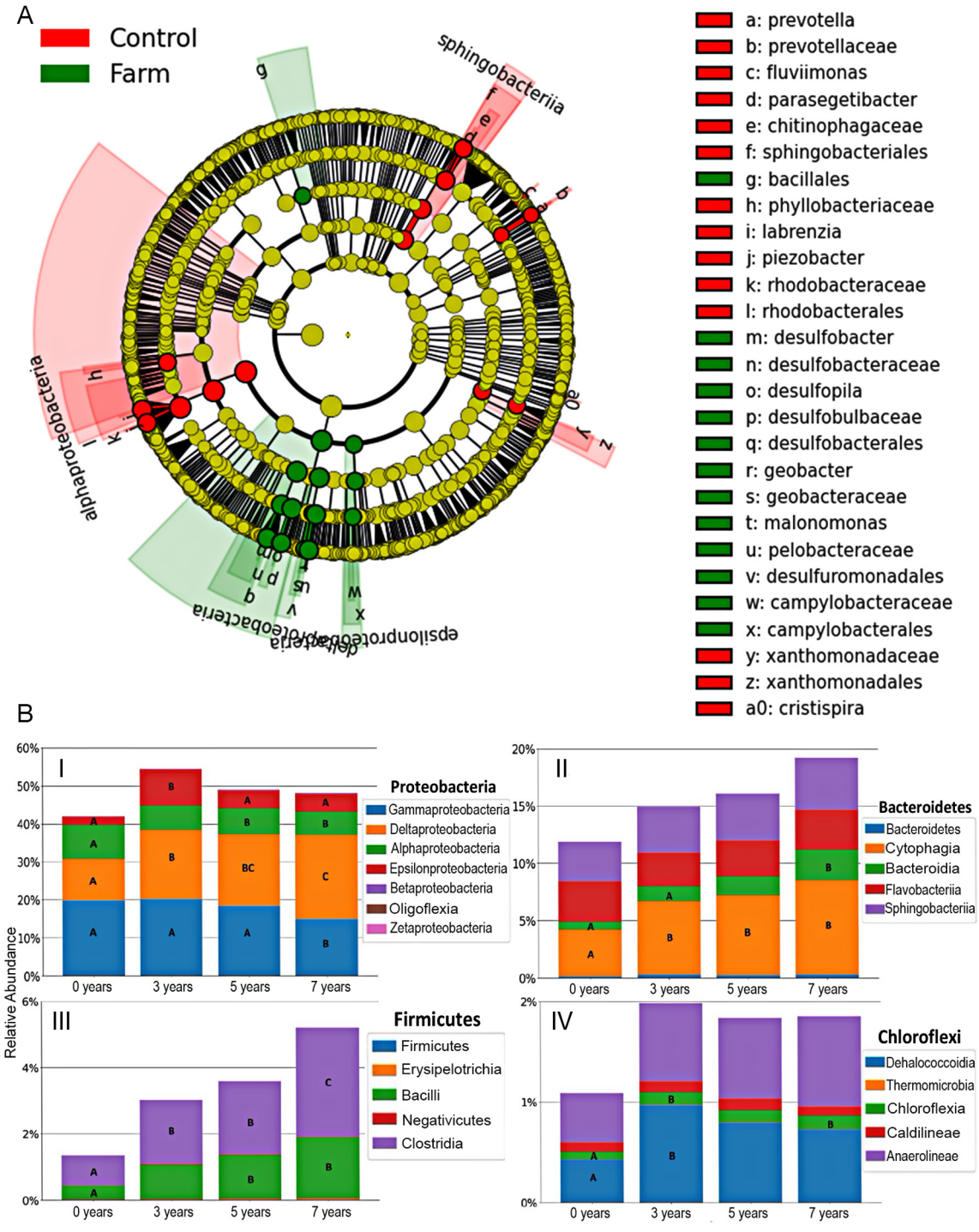

Fig. 2. (A) Linear discriminant analysis effect size (LEfSe) of taxonomic biomarkers at control and 7 yr farm sites and (B) relative abundances of different classes within phylum *Proteobacteria* (I), *Bacteroidetes* (II), *Firmicutes* (III), and *Chloroflexi* (IV). Different letters across the same color bars denote significant differential abundance. Note the different *y*-axis scales

at the other 3 sites. For example, *Nitrospina* (0.08 to 0.21%), *Desulfobacter* (0.06 to 0.57%), *Desulfotignum* (0.04 to 0.50%), *Natranaerovirga* (0.05 to 0.49%), *Desulfopila* (0.07 to 0.39%), *Desulfotalea* (0.18 to 0.78%), *Clostridium* (0.32 to 1.4%), *Bacillus* (0.25 to 1.4%), *Desulfobacterium* (0.71 to 2.6%), *Spirochaeta* (0.44 to 2.9%), *Desulforhopalus* (0.53 to 2.9%), *Draconibacterium* (0.28 to 1.8%), and *Desulfovibrio* (0.39 to 0.78%)

all increased from the control to the 7 yr sites. A few genera also showed greater abundances in the control compared to farmed sites, such as *Cyanobacterium* (5.56 to 13%), *Pseudomonas* (2 to 3.70%), *Acinetobacter* (1.61 to 3.17%) and *Alkanindiges* (0.31 to 0.75%). Another pattern was observed in some rarer genera, where both *Candidatus* Brocadia ($F_{3,30}$ = 6.430, p = 0.003) and *Candidatus* Scalindua ($F_{3,30}$ = 4.237, p = 0.018) showed a nearly 3-fold increase in abundance between control and 7 yr sites.

Principal component analyses (PCAs) of KEGG pathway abundances (from 16S rRNA) showed closer clustering of replicates from the farmed sites compared to controls, with the PCA1 axis explaining 26.6% and PCA2 explaining 9.6% of the variation in abundances (Fig. 3A). PICRUSt revealed 11 KEGG pathways that were statistically different between control and farmed sites, with 8 showing higher (negative fold change) and 3 showing lower enrichment (positive fold change) at farmed compared to control sites (Fig. 3B, p < 0.050). Pathways related to antenna proteins (light-harvesting proteins in aerobic photosynthesis) and steroid biosynthesis were depleted and pathways associated with N-glycan biosynthesis, basal transcription factor, and mTOR signaling were among the top pathways enriched at farm sites compared to control sites. Using 16S rRNA data to predict community function is limited, as putative pathways can be predicted merely due to bacteria containing distant homologs of enzymes important in that pathway, although the pathway itself is not existent in bacteria (Langille et al. 2013). Further, using PICRUSt can overrepresent the presence of human-related pathways due to biases inherent in its biomedical-focused microbial databases. Therefore, observations from community RNA analyses are essential to further validate these functional changes.

3.2. RNA community structure and function

Illumina HiSeq sequencing of extracted RNA generated an average of 28 084 426 ± 12 404 398 RNA sequences in all 6 samples (2 treatments [control vs. 7 yr] × 3 replicates; Table 1). No significant difference between RNA yield, RNA quality, or sequences were

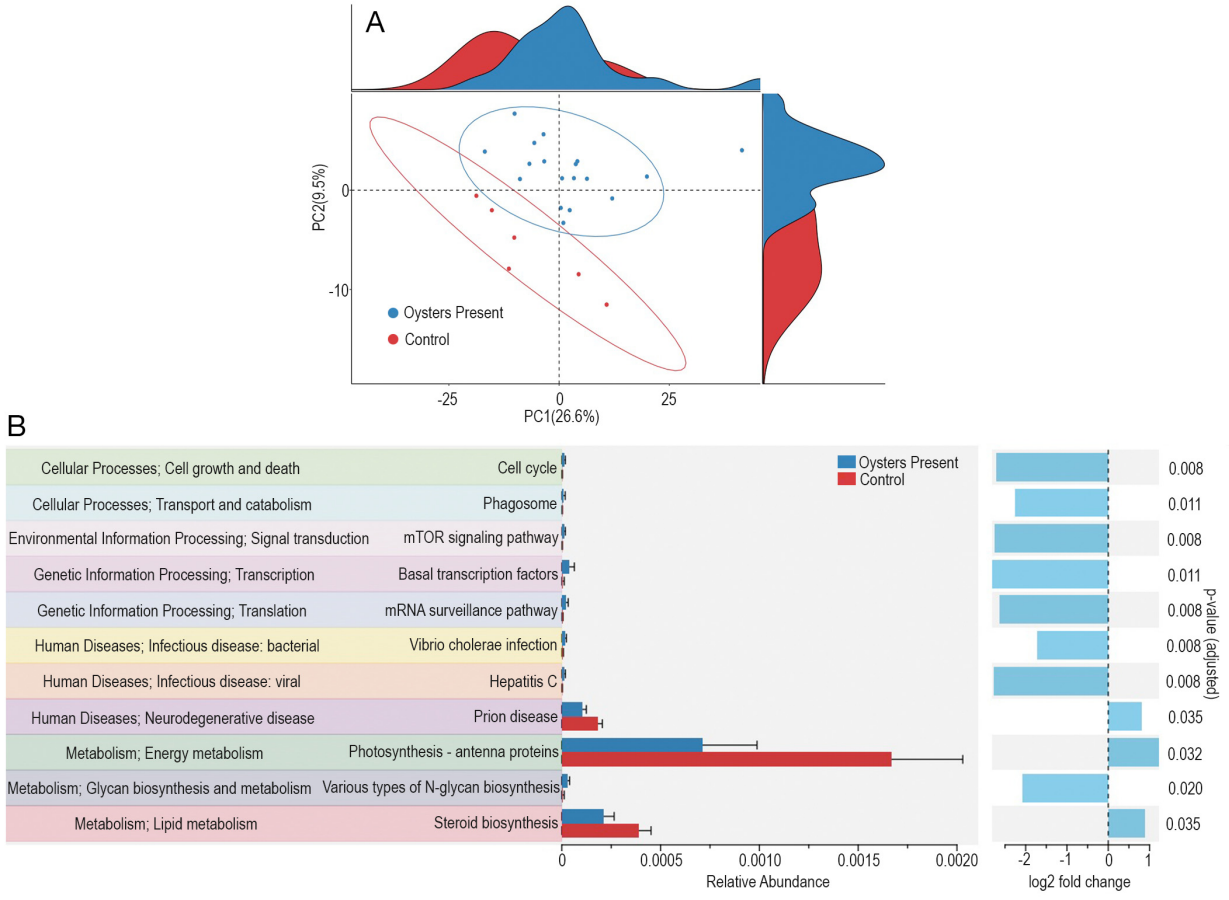

Fig. 3. Functional diversity of the 16S rRNA bacterial community at control and oyster farms: (A) principal component analyses and (B) relative abundances and $\log_2$ fold change of differentially enriched KEGG-annotated pathways

observed between treatment groups ($p > 0.05$). We found that 5459 transcripts were annotated by KEGG that showed no separation in nMDS ordination (Fig. 4A), supported by PERMANOVA that indicated no differences between control or 7 yr site (pseudo-$F_{2,5} = 0.2682$, $p = 0.933$). Differential analyses indicated that 8 genes were upregulated and 18 genes were downregulated in the 7 yr site compared to control (Fig. 4B). Among the transcripts downregulated at the farm sites compared to control, several belonged to gluconeogenesis and the bacterial chemotaxis pathway and 1–2 transcripts to phosphotransferase, glutamate, alanine, and pyruvate metabolic pathways (Fig. 4C). Multiple pathways related to

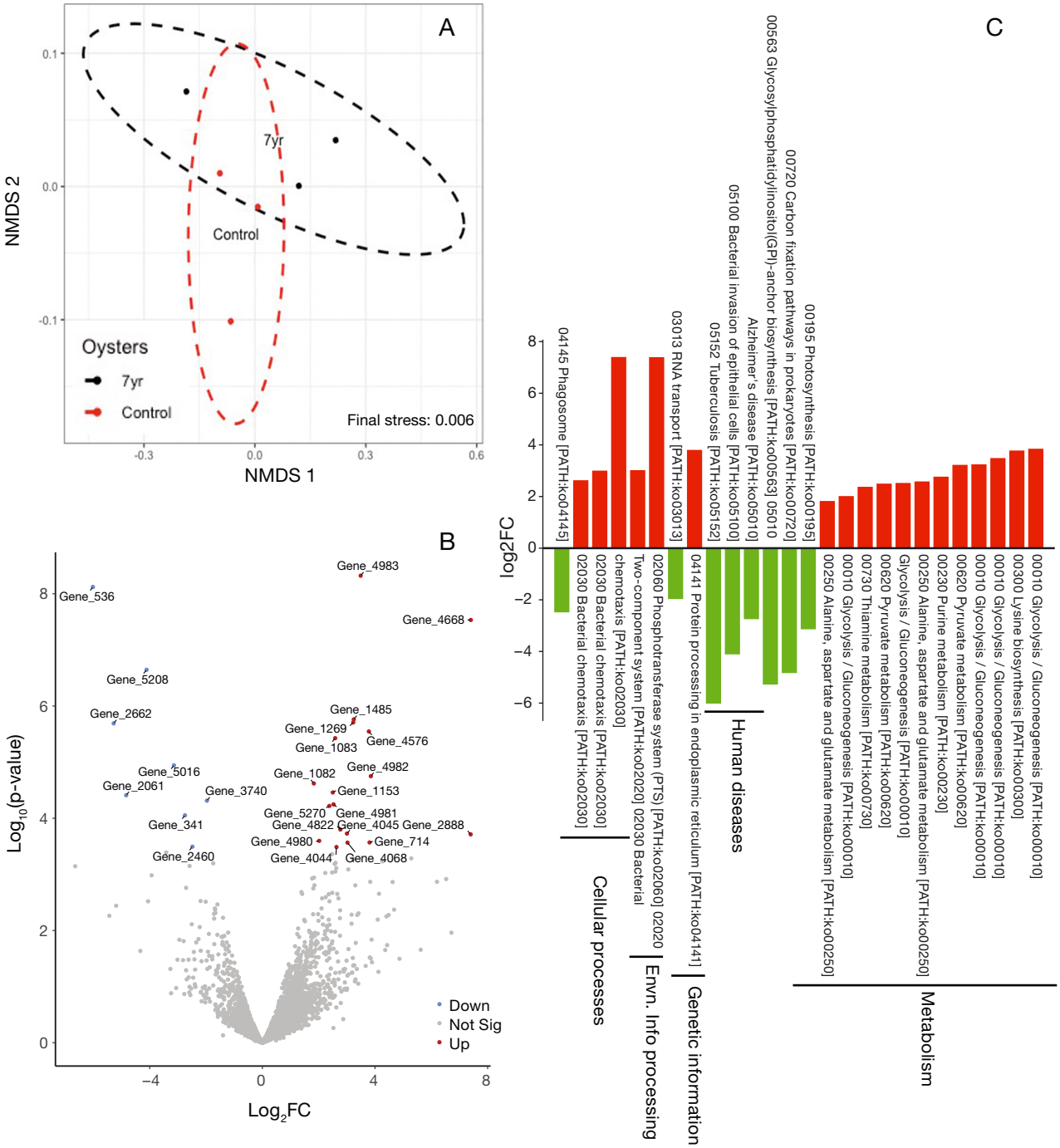

Fig. 4. (A) Non-metric multidimensional scaling (nMDS), (B) volcano plot of the significant differentially expressed RNA transcripts between control and 7 yr sites, and (C) barplot of the differentially expressed KEGG pathways between control and 7 yr sites

human diseases, phagosomes, and C fixation were upregulated in the 7 yr farm sites. We annotated our rRNA transcripts with RefSeq in MG-RAST to compare differences in taxonomic assignments from 16S rRNA amplicon (resident community) and protein-coding reads (active community). We detected a total of 28 and 592 bacterial phyla and genera respectively. nMDS ordination followed by PERMANOVA on bacterial genera showed no separation between control and 7 yr sites (Fig. 5A, pseudo-$F_{2,5}$ = 1.339, p = 0.217). Diversity analyses on genera also did not show any variation between control and 7 yr farm sites (Fig. 5B, Student's *t*-test, p > 0.050). Similar to 16S rRNA amplicons, the top 3 abundant phyla were *Proteobacteria*, *Firmicutes*, and *Bacteroidetes*, followed by *Actinobacteria*, *Cyanobacteria*, *Planctomycetes*, and *Cloroflexi* (Fig. 5C). Eleven out of 28 phyla showed a significant increase in farm sites compared to control that included *Proteobacteria*, *Spirochaetes*, and *Thermotogae* among the most abundant ones. Only *Planctomycetes* showed a significantly greater abundance at control sites. We found that 141 genera showed differ-

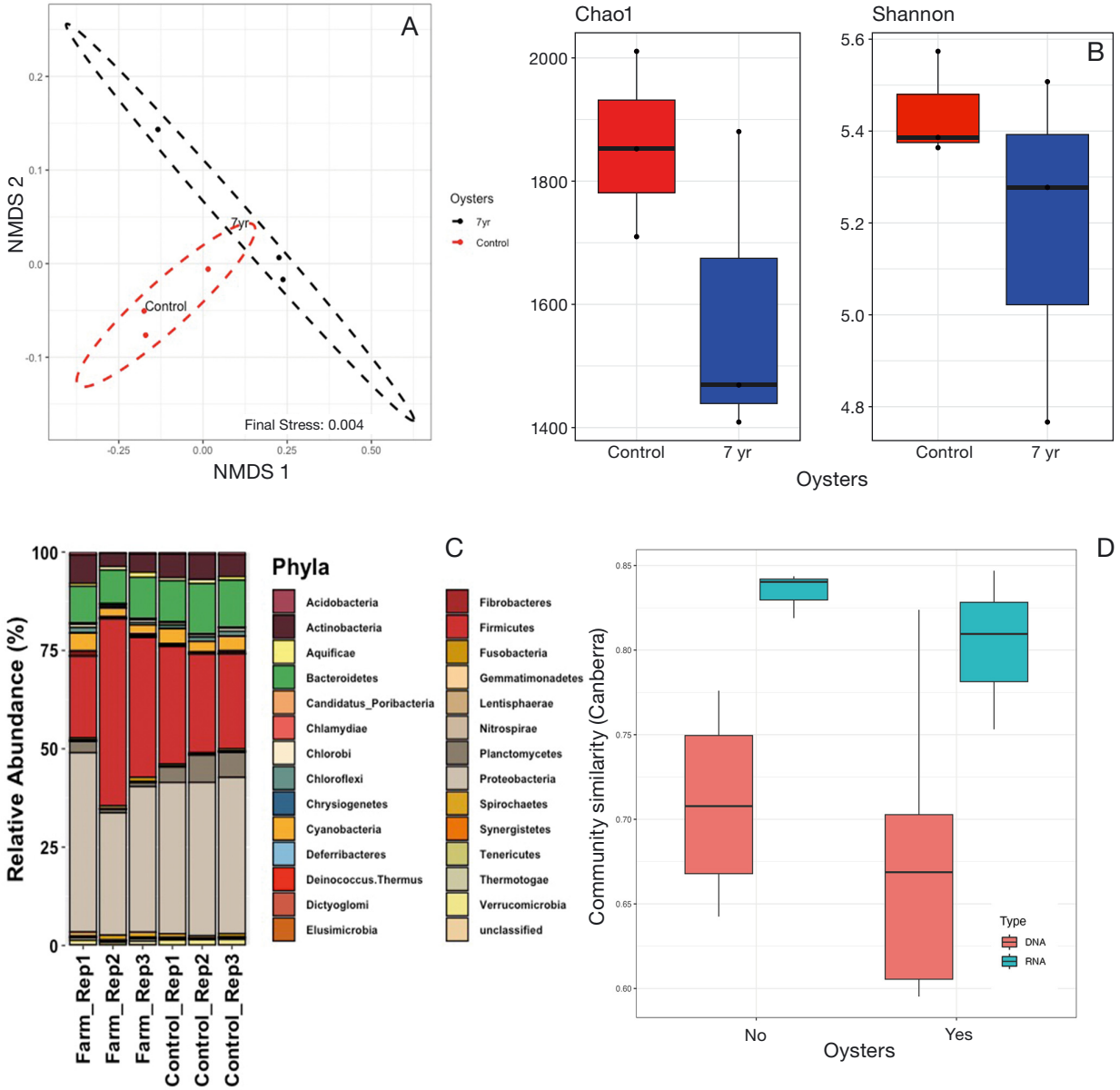

Fig. 5. (A) Non-metric multidimensional scaling (nMDS), (B) Chao1 and Shannon diversity analyses, (C) relative abundances of bacterial phyla in RefSeq-annotated RNA transcripts from control and 7 yr sites, and (D) average pairwise similarity (1 − Canberra distance) of the RNA and 16S rRNA amplicon-inferred communities at control ('No oysters') and 7 yr sites ('Yes oysters'). Student's *t*-test was used to calculate differences between communities (p < 0.001). Boxplot features as in Fig. 1

ential abundance at control and farmed sites (Student's *t*-test, $p < 0.050$), with 124 more abundant at farmed sites and 17 more abundant at control. Supporting 16S rRNA amplicon observations, we saw an increase in *Deltaproteobacteria*, *Epsilonproteobacteria*, and *Firmicutes* and a decrease in *Alphaproteobacteria* and *Gammaproteobacteria* at the farm sites compared to control. In addition, the RNA-derived community showed an increase of *Actinobacteria* and *Betaproteobacteria* in the farmed sites and increase of *Planctomycetes* and *Flavobacteria* in the control. Pairwise comparison of the community distance matrices indicated that DNA- and RNA-derived communities were significantly different at the phylum level at both control and farm sites (Fig. 5D, Control: $t = 7.64$, $p < 0.001$; Farm: $t = 3.630$, $p < 0.010$; Welch 2-sample *t*-test).

3.3. Sediment geochemistry

Twenty elements, excluding hydrogen (H) and oxygen (O), were detected in all 4 sites (Fig. 6, Table S1). nMDS ordination on *z*-transformed concentrations showed closer clustering between control and 5 yr farmed sites, but the former grouped separately from both 3 and 7 yr sites (Fig. 4A). PERMANOVA indicated a significant difference between sites (pseudo-$F_{3,23} = 3.349$, $p = 0.009$), primarily driven by the differences between the control and the 3 yr site ($p = 0.020$). To identify elements that accounted for these site-specific differences, we performed univariate ANOVAs for individual elements across all 4 sites (Fig. 6B). Twelve out of 20 elements (aluminum [Al], potassium [K], P, Cr, Mn, Fe, Co, Ni, Zn, barium [Ba], Cd, and Pb) showed significant differences in concentrations between sites, where all elements except Zn were lower at the 3 yr site compared to control. Approximately half of the elements (11 out of 20 elements: P, Al, K, Cr, Mn, Fe, Co, Zn, Ni, Ba, and Pb) showed significant decreases in concentration at the 7 yr site compared to control. The 3 and 5 year sites varied in 6 out of 20 elements (Mn, Fe, Co, Ni, Pb, and Cr), and the 5 and 7 year sites varied in 4 out of 20 elements (Co, Ni, Ba, and Pb). No elements showed differences in concentrations between control and the 5 yr site, and only Mn showed significant increase at the 7 yr site compared to the 3 yr site.

To better understand the relationship between bacterial community and sediment elemental concentrations, Pearson correlation analysis was done to test for collinearity between elements with each other (Fig. S5A) and with bacterial phyla (Fig. S5B). Calcium (Ca) was negatively correlated to all elements except Cu. Ni, Cr, Mn, Co, Fe, K, and Al showed the strongest positive correlation with each other compared to the rest (Fig. S5A). No overall pattern in collinearity was observed between elements and bacterial phyla (Fig. S5B). The Pearson correlation coefficient (r) varied from −0.1 to +0.64, with only *Cyanobacteria* showing a strong positive correlation (>0.3) with K, Co, Ni, and Ba. The phyla *Proteobacteria*, *Chloroflexi*, *Fusobacteria*, *Ignavibacteriae*, *Acidobacteria*, *Firmicutes*, and *Nitrospinae* showed higher negative r-values (>0.3) with correlated elements Cr, Mn, Fe, and Co. K and Ba also showed strong negative correlation with most phyla. db-RDA was done to test for correlation of elements with bacterial abundances (Fig. 6C). To check for homogeneity of the bacterial data, we first did a de-trended correspondence analysis (1st axis length = 1.14; Lepš & Šmilauer 2003) followed by PCA with the 'envfit' function to test for significance. Al, K, Cr, Mn, Fe, Co, Ni, Zn, and Ba showed a significant p-value (<0.010) and were used for subsequent redundancy analyses (Table S2). RDA1 and RDA2 together explained 32% of abundance variability (Fig. 6C). Al ($p = 0.004$) and Mn ($p = 0.025$) made a significant contribution to the total variation of bacterial community structure.

4. DISCUSSION

In this study, we investigated the impact of oyster farming on bacterial community structure and function. We found that bacterial communities in oyster farm sediments differed significantly from unfarmed sediments (Figs. 1 & 2). Importantly, we did not find any difference in bacterial communities with respect to farming duration (Figs. 1 & 2). In fact, both diversity analyses and LEfSe suggest that several bacterial taxa and genera varied in abundances between the control and the farmed sites, but not between the 3, 5, and 7 yr sites. These results indicate that sediment bacterial communities responded to the pressure of aquaculture within 3 yr, and that this response persisted over time. Although limited to a single farm, the general lack of change in bacterial communities with farming duration could be due to early and rapid reorganization following the introduction of oyster-induced selection pressures, as observed in studies with similar time frames in marine (Simon et al. 1999), freshwater (Hall et al. 2008, 2011), and terrestrial systems (Bradford et al. 2008, DeAngelis et. al. 2010).

Microbial community structure tracks environmental changes due to high adaptation rates (Graham et

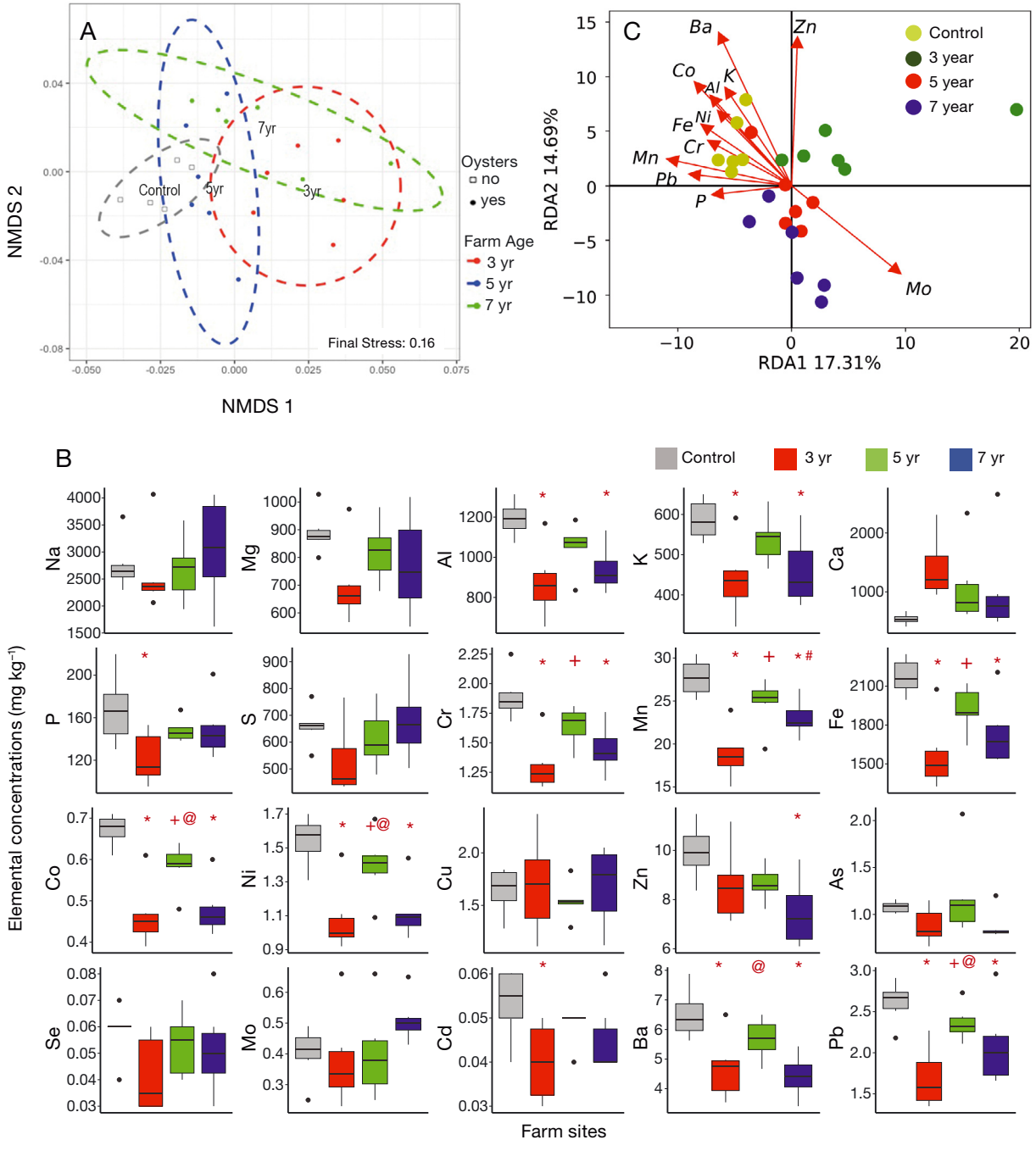

Fig. 6. (A) Non-metric multidimensional scaling (nMDS) of elemental concentrations across control, 3, 5, and 7 yr sites. (B) Concentrations of individual elements across all 4 sampling sites (n = 6). Boxplot features as in Fig. 1. (*): significant differences in elements between the respective farm and control sites; (+): differences between the 3 and 5 yr sites; (@): differences between 5 and 7 yr sites; and (#): differences between 3 and 7 yr sites (Tukey's post hoc; $p < 0.05$). Note the different y-axis scales. (C) Biplot of redundancy analysis (RDA) axes 1 and 2 for bacterial operational taxonomic units with sediment elemental concentrations

al. 2016, Morris et al. 2020). As such, microbial communities are increasingly used as indicators to estimate the environmental impacts of anthropogenic activities in different ecosystems (Paerl et al. 2003, Liao et al. 2018, Schloter et al. 2018). Aquaculture can impact ecosystem biogeochemistry in several ways, such as decreasing oxygen concentrations (Lavoie et al. 2016), increasing sulfide accumulation (Holmer et al. 2005), and enhancing nutrient availability (Carlsson et al. 2012). The presence and absence of certain

microbes can indicate the dominant *in situ* decomposition processes related to these cycles, which in turn can shed light on overall coastal ecosystem quality (Aylagas et al. 2017). Further, the low cost of environmental DNA metabarcoding and the ability to simultaneously record community-level changes in both structure and function makes microbial indicators effective for long-term monitoring of disturbed habitats. In this study, we identified several bacterial taxa that had consistently higher abundance at farmed sites (Figs. 2 & 5). Notable among them is the genus *Spirochaeta*, primarily composed of anaerobes found within sediments exposed to aquaculture (Lin et al. 2015, Verhoeven et al. 2016), and the class *Clostridia*, which are anaerobic species commonly found in soils (Wells & Wilkins 1996). Additionally, LEfSe (Fig. 2) analyses showed increased LDA scores for sulfate-reducing anaerobic *Deltaproteobacteria*, chemolithotrophs associated with *Epsilonproteobacteria*, and facultative anaerobes *Bacillales* in the farmed sites. A higher LDA for *Rhodobacterales* (*Alphaproteobacteria*) that are all strictly aerobic was observed at the control site (Fig. 2). RNA-derived sequences also showed increase of the anaerobic *Thermotogae* phylum at farmed sites. Ray et al. (2020) reported an initial stimulation of sediment O_2 consumption following the introduction of oyster aquaculture, followed by a return to baseline conditions after 7 yr. The observed increase in abundance of microbes that prefer or require anaerobic conditions in our study coupled with past evidence for reduced oxygen availability in sediments under oyster farms suggest a shift towards increased tolerances for anoxia in oyster farm sediment microbes. The contribution of community shifts vs. functional shifts towards such increased tolerances under oyster cages requires further investigations in additional systems to identify specific taxa or precise molecular mechanisms that are at play.

Oysters play a crucial role in mediating microbial-driven N sediment cycling in estuarine systems. At this site, Ray et al. (2020) demonstrated that sediments switched from net N fixation (i.e. N_2 sink) to net denitrification (i.e. net N_2 source) following the establishment of oyster farming. Ray & Fulweiler (2020) also observed a seasonal impact on N fixation and release rates at these sites. N_2 can be produced via canonical denitrification, the microbial conversion of nitrate to N_2, or through anaerobic ammonium oxidation (anammox), which couples NH_4^+ oxidation with NO_2^- reduction to produce N_2. Ray et al. (2020) could not describe the pathway leading to enhanced N_2 production, as they only measured net rates. Our analysis of the microbial community and function can help suggest some mechanisms behind the observed change in net N_2 exchange between sediments and the water column. Here, we see enrichment of few bacterial genera associated with denitrification (e.g. *Bacilli*) and greater abundance of several anaerobic ammonium-oxidizing bacteria (AAOB) capable of anammox, including the genera *Candidatus* Brocadia and *Candidatus* Scalindua at the 7 yr farm site compared to control (Kartal et al. 2008, Awata et al. 2013, Bai et al. 2015). We also did not see enrichment of bacteria commonly associated with the denitrification processes at the oyster farms (e.g. *Alphaproteobacteria*, *Gammaproteobacteria*, and *Chloroflexi*) (Wang et al. 2016). *Nitrospinae* was the only NO_2^--oxidizing bacterial phylum that was consistently more abundant at all farmed sites. Taken together, these data suggest that anammox may have been dominating the N_2 signal at the farmed sites, potentially because rates of nitrification were lower due to reduced O_2 availability. Arfken et al. (2017) quantified differences in bacterial communities across the digestive system, shell, and sediment in an oyster reef and found that genes associated with denitrification were mostly found in the oyster digestive system and on the shell as opposed to in the sediments, further supporting the potential for annamox to dominate N-removal in oyster-impacted sediments. We also observed enrichment of the phyla *Proteobacteria*, *Firmicutes*, and *Spirochaetes* at farmed sites. These phyla include taxa with ability to fix N (Zehr et al. 2003, Delmont et al. 2018). Fulweiler (2023) indicated that N_2 fixation can happen for several reasons, including (but not limited to) maintaining redox balance in cells and increased mineralization of recalcitrant C. The control site showed enrichment of *Alphaproteobacteria* and *Gammaproteobacteria*, both associated with hydrogenotrophic denitrifiers. RNA sequences also showed greater abundance of *Planctomycetes* that has recently been associated with both N_2 fixing (Delmont et al. 2018) as well as anammox (Wiegand et al. 2018). Although the presence and relative contributions of these taxa in driving N-cycle transformations requires further investigations in additional aquaculture farms, our data draws attention to the presence of potentially different microbial taxa and processes dominating the N-cycle at control versus farmed sites.

Previous studies showed changes in abundance of S-cycling bacteria at aquaculture farms (Asami et al. 2005, Rubio-Portillo et al. 2019) due to increased anaerobic reduction of sulfates leading to accumulation of H_2S (Hargrave et al. 1997). LEfSe indicated an overall enrichment of bacterial classes that play significant roles in S cycling, such as *Epsilonproteobactera* and *Deltaproteobacteria* at the farm sites (Fig. 2). Bacterial

orders commonly associated with sulfate reduction (e.g. *Desulfobacterales* and *Desulfuromonadales*) within the class *Deltaproteobacteria* also showed greater enrichment at the farmed sites. Additionally, several S-oxidizing genera (*Desulfopila*, *Desulfotalea*, and *Desulfovibrio*) and S-reducing genera (*Desulfobacter* and *Desulfotignum*) (Kuever 2014) showed greater abundances at farm sites. There is also evidence that oysters may promote sediment PO_4^{3-} regeneration, but at our sampling site, this was not the case (Ray et al. 2020). All 3 farm sites showed a decrease in sediment P compared to control (Fig. 6B). Except for an increase in the genus *Bacillus*, which includes multiple species with the ability to solubilize inorganic phosphates (PSB) (Fig. 2 [16S rRNA] and Fig. 5 [RNA]), we found no other taxa that contribute to the coastal P-cycle at any sites (Calvo et al. 2010, Malfanova et al. 2011, Wahyudi et al. 2011). Remineralization of sediment phosphate is a complex process and is tightly coupled with the C:P ratio of the organic substrate (Scott et al. 2012). Increase in OM deposition by oysters in this site can increase the C:P ratio, slowing the remineralization rates of P at farm sites.

Overall, bacterial community composition varied between DNA (resident) and RNA (active) derived sequences (Fig. 5D). Both provided similar estimates of the abundant phyla, except *Actinobacteria*, that were overrepresented in the RNA sequences (Figs. 2B & 5C), possibly suggesting their increased metabolic activity relative to other groups. Analyzing the RNA-derived community helped us detect changes in the active community separate from changes in community abundances. For example, RNA sequences showed a greater abundance of *Planctomycetes* in the control site, that contains many species capable of anammox (Wiegand et al. 2018). 16S amplicons showed no such enrichment, indicating that although the abundances did not vary between the sites, greater transcriptional efficiency of this group can lead to an active anammox pathway for N_2 production in the control site. Several taxa showed similar trends in both 16S rRNA- and RNA-derived community (e.g. *Proteobacteria*, *Spirochaetes*, *Clostridia)*, but we also observed taxa that showed no differential abundances in the former but significant differences between sites in the latter (e.g. *Flavobacteria*, *Betaproteobacteria*), suggesting that differences in transcriptional rates can contribute to changes in community structure that cannot be predicted from DNA sequences alone. However, compared to 16S rRNA taxonomic assignments, RNA transcripts have very limited capacities to predict distribution of rarer taxa in the sediments. Although both sequence data are biased towards certain groups that are overrepresented in the respective databases, our data indicates that bacterial community indices/biomarkers can be potentially used to predict the impact of oyster farming on estuarine systems, as previously proposed (Asami et al. 2005, Rubio-Portillo et al. 2019).

Our second objective was to identify the functional status of the microbial community, as changes in functional gene transcripts are good indicators of changes in biogeochemical functions (Moran 2009). Shifts in community structure as seen in the present study (Fig. 1) likely affect the functional capacities of sediments, which in turn can bear significant ecological consequences. Both 16S rRNA and RNA sequences were annotated with the same KEGG database, but no similarity in annotations were observed between the two. No overarching patterns were observed between both DNA- and RNA-inferred bacterial functions between our control and 7 yr sites (Figs. 3 & 4). In addition to the inherent variability and the fast turnover rates of mRNA (de Jong et al. 2019), the small sample size (control vs. 7 yr) for RNA transcripts and the limitations of predicting functions from 16S rRNA amplicons may have contributed to the lack of a general pattern across sites. However, when looking at expression of individual genes, several were differentially expressed between control and farm sites. We saw a relative increase in abundances of transcripts for antenna proteins that mediate aerobic photosynthesis and transcripts for oxygen-dependent steroid biosynthesis (Hoshino & Gaucher 2021), supporting the presence of aerobic conditions at the control site compared to the farmed sites. Enrichment of glutamate (containing assimilated ammonia) and alanine pathways at the control site indicates increased assimilation of N (Merrick & Edwards 1995) that is also supported by the increase of *Gammaproteobacteria* and *Planctomycetes* at these sites. Several transcripts involved in glucose production, phosphate metabolism, and bacterial chemotaxis were also enriched at the control site. The increased organic load and increased inorganic N availability (Ray et al. 2020) at the oyster farm probably led to the enrichment of several C biosynthesis pathways such as N-glycan biosynthesis and C fixation. Several human-related pathways (e.g. human disease, phagosomes, basal transcription factors, mTOR signaling) were also enriched, probably indicating a higher degree of anthropogenic disturbances at these farmed sites. For both 16S rRNA and RNA data, we were not able to detect changes in genes directly linked to N, S, and/or anaerobic respiration processes. Adequate sequencing depth and improved taxonomic classification of rare species is nec-

essary to identify effective functional indicators of change at oyster farms.

Oyster aquaculture can impact elemental concentrations of several metals in sediments due to the correlated nature of most biogeochemical cycles (Tovar et al. 2000, Rožič et al. 2012; our Fig. S5). Some studies have indicated a greater concentration of heavy metals (e.g. Cd, Cu, Pb, Zn) in the sediments beneath aquaculture gear due to addition of farm food and increased fecal deposits (Smith et al. 2005, Mendiguchía et al. 2006, Sutherland et al. 2007), while others have not reported similar effects (Basaran et al. 2010, Russell et al. 2011, Rožič et al. 2012). We predicted higher metal concentrations at farm sites, but instead observed a decrease in most elements at the 3 and 7 yr sites compared to the control and the 5 yr site (Fig. 6, Table S1). The differences were mostly driven by higher concentrations of the elements K, Cr, Mn, Fe, Co, and Ni at the control and 5 yr sites, which also exhibited a strong positive correlation with each other (Fig. S5). A possible explanation for lower concentrations of several metals beneath aquaculture might be a release of metals to the water column under low O_2 conditions and lower pH in the sediment (Foster & Fulweiler 2019). Increased bioaccumulation in the oysters could also account for reduction in farm sediments, although further research on somatic measurements from the oysters themselves is essential to test for such associations (Ke & Wang 2001, Azarbad et al. 2010). Previous studies have shown that the accumulation rates in oysters showed little correlation with sediment concentrations, as the former is inherently dependent on the bioavailability of the specific metal that can vary between the sediment and the water column at different sites depending on the physiochemical property of the metal itself (Hayes et al. 1998, Apeti et al. 2005, Chen et al. 2014). For example, Apeti et al. (2005) found that oysters incorporate heavy metals (Cu, Pb, and Zn) mostly from the surrounding water column compared to the sediments and exhibit high spatial variations in accumulation rates. To a certain extent, the similarity of elemental concentrations observed at the control and the 5 yr sites in the present study indicates that factors other than the presence/absence of oysters influence sediment metal concentrations. Along with the geochemical properties of the sediments (Nobi et al. 2010), several anthropogenic sources such as dredging, industrial emissions, and sewage treatments can cause significant variations in concentrations across different sites within the same habitat (Zhang et al. 2014). Although further testing is needed to differentiate between natural and aquaculture-derived differences in sediment concentrations, our data indicate that the effect of oyster farms on increased accumulation of metals is negligible, at least in this coastal system.

Changes in sediment elemental concentrations can alter the resident microbial community, which in turn can drive changes in nutrient cycles (Ni et al. 2016, Wang et al. 2023). For example, heavy metal accumulation in sediments have been shown to inhibit the N cycle and increase sulfate reduction, both processes likely influenced by changes in the resident microbes (Kandeler et al. 1996, Kang et al. 2013). We found several bacterial phyla that correlated with changes in sediment elemental concentrations (Fig. 6B). For example, the positive correlation observed between *Cyanobacteria* with metals such as Co, Ni, and Ba indicates a probable link between these trace metals and their regulation of cyanobacterial growth, as seen in previous studies (Facey et al. 2019). Several Fe- and Mn-oxidizing bacterial taxa are commonly associated with the phyla *Proteobacteria* and *Acidobacteria*, which could be the reason for the strong correlation observed here. Although causal relationships are highly complicated and require further investigations into metal bioavailability, our data highlights the importance of considering sediment geochemistry in shaping the resident microbial community. Redundancy analyses revealed that the elements Al, K, Cr, Mn, Fe, Co, Ni, Zn, and Ba together explained 32% of the bacterial community variations across sites (Fig. 6). Al and Mn showed the highest impact, lending support to the established role of Mn in shaping microbial communities (Algora et al. 2015, Wang et al. 2024). To our knowledge, our study is the first to demonstrate the correlation between several other metal concentrations and estuarine bacterial composition, supporting similar observations in river systems (Yang et al. 2013, Zhang et al. 2016). Anthropogenic pollution can increase influxes of most of these elements, including Al and Mn, into estuarine systems (Ansari et al. 2004, Botté et al. 2022), which in turn could significantly modify the sediment bacterial communities, with potential ecological consequences.

5. CONCLUSION

Our study used a multi-omics approach to identify changes in the structure and function of sediment microbial communities and associated changes in sediment elemental concentrations across a chronosequence (space-for-time substitution) in a commercial oyster farm in Ninigret Pond, Rhode Island. Our

results indicate significant changes in both the structure and function of bacterial communities between the control and farm sites, but this change is not affected by the duration of farming, at least up to 7 yr as indicated here. We identified several taxa that shifted abundance in response to oysters, and with further testing at additional sites, could potentially serve as indicators of the impacts of farming on estuarine sediment communities. Differences in bacterial functions between control and farm sites were less pronounced. We found no evidence of heavy metal accumulation under the oyster cages, indicating a trivial effect of farming on sediment metal concentrations. It is, however, important to note that the current study is limited to a single oyster farm, and further investigations at additional farm locations are warranted to establish common patterns in sediment processes. Nonetheless, this study provides a comprehensive account of both short- and long-term impacts of oysters on estuarine sediments and highlights the importance of considering the correlated effects of such shifts while predicting the ecological impacts of these practices within these habitats.

Data availability. The 16S rRNA gene amplicon and RNA sequences have been uploaded to the DDBJ Sequence Read Archive (SRA) under accession no. PRJNA561593. (https://www.ncbi.nlm.nih.gov/sra/?term=PRJNA561593)

Acknowledgements. This research was funded, in part, by a grant to R.W.F. from RI Sea Grant and a grant to P.R.C. from NH-INBRE (NIH grant no. 5P20GM103506-09, subaward agreement no. R1040). We thank Joseph Owens from Keene State College for sample preparation and Tim Maguire and Gabrielle Hillyer from Boston University for assistance with field sampling.

LITERATURE CITED

Algora C, Vasileiadis S, Wasmund K, Trevisan M, Krüger M, Puglisi E, Adrian L (2015) Manganese and iron as structuring parameters of microbial communities in Arctic marine sediments from the Baffin Bay. FEMS Microb Ecol 91:fiv056

Ansari TM, Marr IL, Tariq N (2004) Heavy metals in marine pollution perspective — a mini review. J Appl Sci 4:1–20

Apeti DA, Robinson L, Johnson E (2005) Relationships between heavy metal concentrations in the American oyster (*Crassostrea virginica*) and metal levels in the water column and sediment in Apalachicola Bay Florida. Am J Environ Sci 1:179–186

Arfken A, Song B, Bowman JS, Piehler M (2017) Denitrification potential of the eastern oyster microbiome using a 16S rRNA gene based metabolic inference approach. PLOS ONE 12:e0185071

Asami H, Aida M, Watanabe K (2005) Accelerated sulfur cycle in coastal marine sediment beneath areas of intensive shellfish aquaculture. Appl Environ Microbiol 71: 2925–2933

Awata T, Oshiki M, Kindaichi T, Ozaki N, Ohashi A, Okabe S (2013) Physiological characterization of an anaerobic ammonium-oxidizing bacterium belonging to the '*Candidatus* Scalindua' group. Appl Environ Microbiol 79: 4145–4148

Aylagas E, Borja Á, Tangherlini M, Dell'Anno A, Corinaldesi C, Michell CT, Rodríguez-Ezpeleta N (2017) A bacterial community-based index to assess the ecological status of estuarine and coastal environments. Mar Pollut Bull 114: 679–688

Azarbad H, Khoi AJ, Mirvaghefi A, Danekar A, Shapoori M (2010) Biosorption and bioaccumulation of heavy metals by rock oyster *Saccostrea cucullata* in the Persian Gulf. Int Aquat Res 2:61

Bai R, Chen X, He JZ, Shen JP, Zhang LM (2015) *Candidatus* Brocadia and *Candidatus* Kuenenia predominated in anammox bacterial community in selected Chinese paddy soils. J Soils Sediments 15:1977–1986

Basaran AK, Aksu M, Egemen O (2010) Impacts of the fish farms on the water column nutrient concentrations and accumulation of heavy metals in the sediments in the Eastern Aegean Sea (Turkey). Environ Monit Assess 162: 439–451

Beck MW, Brumbaugh RD, Airoldi L, Carranza A, Coen LD, Crawford C, Guo X (2011) Oyster reefs at risk and recommendations for conservation restoration and management. Bioscience 61:107–116

Bolger AM, Lohse M, Usadel B (2014) Trimmomatic: a flexible trimmer for Illumina sequence data. Bioinformatics 30:2114–2120

Bolyen E, Rideout JR, Dillon MR, Bokulich NA and others (2019) Reproducible interactive scalable and extensible microbiome data science using QIIME 2. Nat Biotechnol 37:852–857

Boothe PN, Knauer GA (1972) The possible importance of fecal material in the biological amplification of trace and heavy metals. Limnol Oceanogr 17:270–274

Botta R, Asche F, Borsum JS, Camp EV (2020) A review of global oyster aquaculture production and consumption. Mar Policy 117:103952

Botté A, Zaidi M, Guery J, Fichet D, Leignel V (2022) Aluminum in aquatic environments: abundance and ecotoxicological impacts. Aquat Ecol 56:751–773

Bouwman J, Kiewiet J, Lindenbergh A, Van Eunen K, Siderius M, Bakker BM (2011) Metabolic regulation rather than de novo enzyme synthesis dominates the osmo-adaptation of yeast. Yeast 28:43–53

Bradford MA, Davies CA, Frey SD, Maddox TR and others (2008) Thermal adaptation of soil microbial respiration to elevated temperature. Ecol Lett 11:1316–1327

Burgin AJ, Yang WH, Hamilton SK, Silver WL (2011) Beyond carbon and nitrogen: How the microbial energy economy couples elemental cycles in diverse ecosystems. Front Ecol Environ 9:44–52

Calvo P, Ormeño-Orrillo E, Martínez-Romero E, Zúñiga D (2010) Characterization of *Bacillus* isolates of potato rhizosphere from Andean soils of Peru and their potential PGPR characteristics. Braz J Microbiol 41:899–906

Caporaso JG, Lauber CL, Walters WA, Berg-Lyons D, Lozupone CA, Turnbaugh PJ, Knight R (2011) Global patterns of 16S rRNA diversity at a depth of millions of sequences per sample. Proc Natl Acad Sci USA 108:4516–4522

Carlsson MS, Engström P, Lindahl O, Ljungqvist L,

Petersen JK, Svanberg L, Holmer M (2012) Effects of mussel farms on the benthic nitrogen cycle on the Swedish west coast. Aquacult Environ Interact 2:177–191

Chen YM, Li HC, Tsao TM, Wang LC, Chang Y (2014) Some selected heavy metal concentrations in water sediment and oysters in the Er-Ren estuary Taiwan: chemical fractions and the implications for biomonitoring. Environ Monit Assess 186:7023–7033

Cole JR, Wang Q, Fish JA, Chai B, McGarrell DM, Sun Y, Tiedje JM (2014) Ribosomal Database Project: data and tools for high throughput rRNA analysis. Nucleic Acids Res 42(D1):D633–D642

de Jong TV, Moshkin YM, Guryev V (2019) Gene expression variability: the other dimension in transcriptome analysis. Physiol Genomics 51:145–158

DeAngelis KM, Silver WL, Thompson AW, Firestone MK (2010) Microbial communities acclimate to recurring changes in soil redox potential status. Environ Microbiol 12:3137–3149

Delmont TO, Quince C, Shaiber A, Esen ÖC and others (2018) Nitrogen-fixing populations of *Planctomycetes* and *Proteobacteria* are abundant in surface ocean metagenomes. Nat Microbiol 3:804–813

Edgar RC, Haas BJ, Clemente JC, Quince C, Knight R (2011) UCHIME improves sensitivity and speed of chimera detection. Bioinformatics 27:2194–2200

Facey JA, Apte SC, Mitrovic SM (2019) A review of the effect of trace metals on freshwater cyanobacterial growth and toxin production. Toxins (Basel) 11:643

FAO (Food and Agriculture Organization of the United Nations) (2018) The future of food and agriculture: alternative pathways to 2050. FAO, Rome

Feinman SG, Farah YR, Bauer JM, Bowen JL (2018) The influence of oyster farming on sediment bacterial communities. Estuar Coasts 41:800–814

Fernandes AD, Macklaim JM, Linn TG, Reid G, Gloor GB (2013) ANOVA-like differential expression (ALDEx) analysis for mixed population RNA-Seq. PLOS ONE 8: e67019

Foster SQ, Fulweiler RW (2019) Estuarine sediments exhibit dynamic and variable biogeochemical responses to hypoxia. J Geophys Res Biogeosci 124:737–758

Fulweiler RW (2023) More foxes than hedgehogs: the case for nitrogen fixation in coastal marine sediments. Glob Biogeochem Cycles 37(8):e2023GB007777

Fulweiler RW, Nixon SW, Buckley BA, Granger SL (2007) Reversal of the net nitrogen flux in coastal marine sediments. Nature 448:180–182

Fulweiler RW, Brown SM, Nixon SW, Jenkins BD (2013) Evidence and a conceptual model for the co-occurrence of nitrogen fixation and denitrification in heterotrophic marine sediments. Mar Ecol Prog Ser 482:57–68

Ge X, Vaccaro BJ, Thorgersen MP, Poole FL and others (2019) Iron- and aluminum-induced depletion of molybdenum in acidic environments impedes the nitrogen cycle. Environ Microbiol 21:152–163

Glassing A, Dowd SE, Galandiuk S, Davis B, Jorden JR, Chiodini RJ (2015) Changes in 16s RNA gene microbial community profiling by concentration of prokaryotic DNA. J Microbiol Methods 119:239–242

Graham EB, Knelman JE, Schindlbacher A, Siciliano S, Breulmann M, Yannarell A, Nemergut DR (2016) Microbes as engines of ecosystem function: When does community structure enhance predictions of ecosystem processes? Front Microbiol 7:214

Green DS, Boots B, Crowe TP (2012) Effects of non-indigenous oysters on microbial diversity and ecosystem functioning. PLOS ONE 7:e48410

Hall EK, Neuhauser C, Cotner JB (2008) Toward a mechanistic understanding of how natural bacterial communities respond to changes in temperature in aquatic ecosystems. ISME J 2:471–481

Hall EK, Maixner F, Franklin O, Daims H, Richter A, Battin T (2011) Linking microbial and ecosystem ecology using ecological stoichiometry: a synthesis of conceptual and empirical approaches. Ecosystems 14:261–273

Hargrave BT, Phillips GA, Doucette LI, White MJ, Milligan TG, Wildish DJ, Cranston RE (1997) Assessing benthic impacts of organic enrichment from marine aquaculture. In: Evans RD, Wisniewski J, Wisniewski JR (eds) The interactions between sediments and water: Proc 7th Int Symp, Baveno, Italy 22–25 September 1996. Springer, Dordrecht, p 641–650

Hayes WJ, Anderson IJ, Gaffoor MZ, Hurtado J (1998) Trace metals in oysters and sediments of Botany Bay, Sydney. Sci Total Environ 212:39–47

Holmer M, Wildish D, Hargrave B (2005) Organic enrichment from marine finfish aquaculture and effects on sediment biogeochemical processes. Handb Env Chem 5:181–206

Hoshino Y, Gaucher EA (2021) Evolution of bacterial steroid biosynthesis and its impact on eukaryogenesis. Proc Natl Acad Sci USA 118:e2101276118

Hussain S, Khaliq A, Noor MA, Tanveer M, Hussain HA, Hussain S, Mehmood T (2020) Metal toxicity and nitrogen metabolism in plants: an overview. In: Datta R, Meena RS, Pathan SI, Ceccherini MT (eds) Carbon and nitrogen cycling in soil. Springer, Berlin, p 221–248

Kandeler F, Kampichler C, Horak O (1996) Influence of heavy metals on the functional diversity of soil microbial communities. Biol Fertil Soils 23:299–306

Kang S, Van Nostrand JD, Gough HL, He Z, Hazen TC, Stahl DA, Zhou J (2013) Functional gene array-based analysis of microbial communities in heavy metals-contaminated lake sediments. FEMS Microbiol Ecol 86:200–214

Kartal B, Van Niftrik L, Rattray J, Van De Vossenberg JL and others (2008) *Candidatus* 'Brocadia fulgida': an autofluorescent anaerobic ammonium oxidizing bacterium. FEMS Microbiol Ecol 63:46–55

Ke C, Wang WX (2001) Bioaccumulation of Cd Se and Zn in an estuarine oyster (*Crassostrea rivularis*) and a coastal oyster (*Saccostrea glomerata*). Aquat Toxicol 56:33–51

Kellogg ML, Cornwell JC, Owens MS, Paynter KT (2013) Denitrification and nutrient assimilation on a restored oyster reef. Mar Ecol Prog Ser 480:1–19

Kuever J (2014) The family *Desulfobulbaceae*. In: Rosenberg E, DeLong EF, Lory S, Stackebrandt E, Thompson F (eds) The prokaryotes: *Deltaproteobacteria* and *Epsilonproteobacteria*. Springer, Berlin, p 75–86

Langille MG, Zaneveld J, Caporaso JG, McDonald D and others (2013) Predictive functional profiling of microbial communities using 16S rRNA marker gene sequences. Nat Biotechnol 31:814–821

Lavoie MF, McKindsey CW, Pearce CM, Archambault P (2016) Influence of intertidal Manila clam *Venerupis philippinarum* aquaculture on biogeochemical fluxes. Aquacult Environ Interact 8:117–130

Lepš J, Šmilauer P (2003) Multivariate analysis of ecological data using CANOCO. Cambridge University Press, Cambridge

Liao H, Chapman SJ, Li Y, Yao H (2018) Dynamics of microbial

biomass and community composition after short-term water status change in Chinese paddy soils. Environ Sci Pollut Res Int 25:2932–2941
Lin R, Lin X, Guo T, Wu L, Zhang W, Lin W (2015) Metaproteomic analysis of bacterial communities in marine mudflat aquaculture sediment. World J Microbiol Biotechnol 31:1397–1408
Liu H, Liao Y, Zhang H, Song X, Tang Y, Liu Q, Zeng J (2023) Fish and shellfish aquaculture impact on the sediment bacterial communities in Xiangshan Bay China. Aquacult Res 2023:9199534
Love MI, Huber W, Anders S (2014) Moderated estimation of fold change and dispersion for RNA-seq data with DESeq2. Genome Biol 15:550
Lynum CA, Bulseco AN, Dunphy CM, Osborne SM and others (2020) Microbial community response to a passive salt marsh restoration. Estuar Coasts 43:1439–1455
Malfanova N, Kamilova F, Validov S, Shcherbakov A, Chebotar V, Tikhonovich I, Lugtenberg B (2011) Characterization of *Bacillus subtilis* HC8 a novel plant-beneficial endophytic strain from giant hogweed. Microb Biotechnol 4:523–532
Mendiguchía C, Moreno C, Mánuel-Vez MP, García-Vargas M (2006) Preliminary investigations on the enrichment of heavy metals in marine sediments originated from intensive aquaculture effluents. Aquaculture 254:317–325
Merrick MJ, Edwards RA (1995) Nitrogen control in bacteria. Microbiol Rev 59:604–622
Meyer F, Paarmann D, D'Souza M, Olson R, Glass EM, Kubal M, Edwards R (2008) The metagenomics RAST server — a public resource for the automatic phylogenetic and functional analysis of metagenomes. BMC Bioinform 9:1–8
Meyer KM, Petersen IA, Tobi E, Korte L, Bohannan BJ (2019) Use of RNA and DNA to identify mechanisms of bacterial community homogenization. Front Microbiol 10:2066
Moran MA (2009) Metatranscriptomics: eavesdropping on complex microbial communities. Microbe 4:7
Morris A, Meyer K, Bohannan B (2020) Linking microbial communities to ecosystem functions: what we can learn from genotype–phenotype mapping in organisms. Philos Trans R Soc B 375:20190244
National Marine Fisheries Service (2020) Fisheries of the United States 2018. US Department of Commerce, NOAA Current Fishery Statistics No. 2018. https://www.fisheries.noaa.gov/national/commercial-fishing/fisheries-united-states-2018 (accessed 31 May 2024)
Newell RIE, Cornwell JC, Owens MS (2002) Influence of simulated bivalve biodeposition and microphytobenthos on sediment nitrogen dynamics: a laboratory study. Limnol Oceanogr 47:1367–1379
Ni C, Horton DJ, Rui J, Henson MW, Jiang Y, Huang X, Learman DR (2016) High concentrations of bioavailable heavy metals impact freshwater sediment microbial communities. Ann Microbiol 66:1003–1012
Nijburg JW, Coolen MJL, Gerards S, Klein Gunnewiek PJA, Laanbroek H (1997) Effects of nitrate availability and the presence of *Glyceria maxima* on the composition and activity of the dissimilatory nitrate-reducing bacterial community. Appl Environ Microbiol 63:931–937
Nobi EP, Dilipan E, Thangaradjou T, Sivakumar K, Kannan L (2010) Geochemical and geo-statistical assessment of heavy metal concentration in the sediments of different coastal ecosystems of Andaman Islands, India. Estuar Coast Shelf Sci 87:253–264
Nowicki BL, Nixon SW (1985) Benthic community metabolism in a coastal lagoon ecosystem. Mar Ecol Prog Ser 22: 21–30
Oksanen J, Blanchet FG, Kindt R, Legendre P and others (2013) Package 'vegan'. Community ecology package, version 2(9). https://CRAN.R-project.org/package=vegan
Paerl HW, Dyble J, Moisander PH, Noble RT, Piehler MF, Pinckney JL, Valdes LM (2003) Microbial indicators of aquatic ecosystem change: current applications to eutrophication studies. FEMS Microbiol Ecol 46:233–246
Pettersson K (1998) Mechanisms for internal loading of phosphorus in lakes. Hydrobiologia 373:21–25
Ray NE, Fulweiler RW (2020) Seasonal patterns of benthic–pelagic coupling in oyster habitats. Mar Ecol Prog Ser 652:95–109
Ray NE, Fulweiler RW (2021) Meta-analysis of oyster impacts on coastal biogeochemistry. Nat Sustain 4:261–269
Ray NE, Al-Haj AN, Fulweiler RW (2020) Sediment biogeochemistry along an oyster aquaculture chronosequence. Mar Ecol Prog Ser 646:13–27
Ray NE, Hancock B, Brush MJ, Colden A, Cornwell J, Labrie MS, Fulweiler RW (2021) A review of how we assess denitrification in oyster habitats and proposed guidelines for future studies. Limnol Oceanogr Methods 19:714–731
R Core Team (2017) R: a language and environment for statistical computing. R Foundation for Statistical Computing, Vienna
RStudio Team (2020) RStudio: Integrated Development for R. RStudio, Boston, MA
Richardson NF, Ruesink JL, Naeem S, Hacker SD, Tallis HM, Dumbauld BR, Wisehart LM (2008) Bacterial abundance and aerobic microbial activity across natural and oyster aquaculture habitats during summer conditions in a northeastern Pacific estuary. Hydrobiologia 596:269–278
Rožič PŽ, Dolenec T, Baždarić B, Karamarko V, Kniewald G, Dolenec M (2012) Major, minor and trace element content derived from aquacultural activity of marine sediments (Central Adriatic, Croatia). Environ Sci Pollut Res Int 19:2708–2721
Rubio-Portillo E, Villamor A, Fernandez-Gonzalez V, Antón J, Sanchez-Jerez P (2019) Exploring changes in bacterial communities to assess the influence of fish farming on marine sediments. Aquaculture 506:459–464
Russell M, Robinson CD, Walsham P, Webster L, Moffat CF (2011) Persistent organic pollutants and trace metals in sediments close to Scottish marine fish farms. Aquaculture 319:262–271
Scala DJ, Kerkhof LJ (1999) Diversity of nitrous oxide reductase (*nosZ*) genes in continental shelf sediments. Appl Environ Microbiol 65:1681–1687
Schloter M, Nannipieri P, Sørensen SJ, van Elsas JD (2018) Microbial indicators for soil quality. Biol Fertil Soils 54: 1–10
Schmidt JM, Henken S, Dowd SE, McLaughlin RW (2018) Analysis of the microbial diversity in the fecal material of giraffes. Curr Microbiol 75:323–327
Scott JT, Cotner JB, Lapara TM (2012) Variable stoichiometry and homeostatic regulation of bacterial biomass elemental composition. Front Microbiol 3:42
Segata N, Izard J, Waldron L, Gevers D, Miropolsky L, Garrett WS, Huttenhower C (2011) Metagenomic biomarker discovery and explanation. Genome Biol 12:R60
Silva DDC, Bellato CR, Marques Neto JDO, Fontes MP (2018) Arsenic and trace metals in water and sediment of the Velhas River southeastern Iron Quadrangle region Minas Gerais Brazil. Quim Nova 41:1011–1018

Simon M, Glöckner FO, Amann R (1999) Different community structure and temperature optima of heterotrophic picoplankton in various regions of the Southern Ocean. Aquat Microb Ecol 18:275–284

Smith JN, Yeats PA, Milligan TG (2005) Sediment geochronologies for fish farm contaminants in Lime Kiln Bay, Bay of Fundy. In: Hargrave BT (ed) Environmental effects of marine finfish aquaculture. Springer, Berlin, p 221–238

Stevens JTE, Fulweiler RW, Roy Chowdhury P (2019) 16S rRNA gene amplicon sequencing of sediment bacterial communities in an oyster farm in Rhode Island. Microbiol Resour Announc 8:e01074-19

Sutherland TF, Petersen SA, Levings CD, Martin AJ (2007) Distinguishing between natural and aquaculture-derived sediment concentrations of heavy metals in the Broughton Archipelago, British Columbia. Mar Pollut Bull 54: 1451–1460

Tovar A, Moreno C, Mánuel-Vez MP, García-Vergas M (2000) Environmental impacts of intensive aquaculture in marine waters. Water Res 34:334–342

Urich T, Lanzén A, Qi J, Huson DH, Schleper C, Schuster SC (2008) Simultaneous assessment of soil microbial community structure and function through analysis of the meta-transcriptome. PLOS ONE 3:e2527

Verhoeven JTP, Salvo F, Hamoutene D, Dufour SC (2016) Bacterial community composition of flocculent matter under a salmonid aquaculture site in Newfoundland Canada. Aquacult Environ Interact 8:637–646

Wahyudi AB, Astuti RP, Widyawati A, Meryandini A, Nawangsih AA (2011) Characterization of *Bacillus* sp. strains isolated from rhizosphere of soybean plants for their use as potential plant growth for promoting *Rhizobacteria*. J Microbiol Antimicrob 3:34–40

Wang G, Feng Z, Yin X, Chen D and others (2024) Biogenic manganese oxides promote metal(loid) remediation by shaping microbial communities in biological aqua crust. Water Res 253:121287

Wang R, He J, Wang J (2016) Heterotrophic bacterial abundance and diversity in the farming environment and guts of the oyster *Crassostrea hongkongensis.* J Shellfish Res 35:343–350

Wang T, Ru X, Deng B, Zhang C, Wang X, Yang B, Zhang L (2023) Evidence that offshore wind farms might affect marine sediment quality and microbial communities. Sci Total Environ 856:158782

Wells CL, Wilkins TD (1996) *Clostridia*: sporeforming anaerobic bacilli. In: Baron S (ed) Medical microbiology, 4th edn. University of Texas Medical Branch at Galveston, Galveston, TX, p 1012–1045

Wickham H (2009) ggplot2: elegant graphics for data analysis. Springer-Verlag, New York, NY

Wiegand S, Jogler M, Jogler C (2018) On the maverick *Planctomycetes*. FEMS Microbiol Rev 42:739–760

Yang C, Mai J, Cao X, Burberry A, Cominelli F, Zhang L (2023) ggpicrust2: an R package for PICRUSt2 predicted functional profile analysis and visualization. Bioinformatics 39:8btad470

Yang T, Liu J, Chen Q (2013) Assessment of plain river ecosystem function based on improved gray system model and analytic hierarchy process for the Fuyang River Haihe River Basin China. Ecol Model 268:37–47

Ysebaert T, Walles B, Haner J, Hancock B (2019) Habitat modification and coastal protection by ecosystem-engineering reef-building bivalves. In: Smaal A, Ferreira J, Grant J, Petersen J, Strand Ø (eds) Goods and services of marine bivalves. Springer, Cham, p 253–273

Yu K, Zhang T (2012) Metagenomic and meta transcriptomic analysis of microbial community structure and gene expression of activated sludge. PLOS ONE 7:e38183

Zehr JP, Jenkins BD, Short SM, Steward GF (2003) Nitrogenase gene diversity and microbial community structure: a cross-system comparison. Environ Microbiol 5:539–554

Zhang C, Yu ZG, Zeng GM, Jiang M, Yang ZZ, Cui F, Hu L (2014) Effects of sediment geochemical properties on heavy metal bioavailability. Environ Int 73:270–281

Zhang X, Gu Q, Long XE, Li ZL and others (2016) Anthropogenic activities drive the microbial community and its function in urban river sediment. J Soil Sediment 16: 716–725

Zu Ermgassen PS, Spalding MD, Blake B, Coen LD, Dumbauld B, Geiger S, Brumbaugh R (2012) Historical ecology with real numbers: past and present extent and biomass of an imperiled estuarine habitat. Proc R Soc B 279: 3393–3400

Editorial responsibility: Brett Dumbauld, Newport, Oregon, USA
Reviewed by: 3 anonymous referees

Submitted: January 27, 2024
Accepted: August 7, 2024
Proofs received from author(s): December 1, 2024